Impact of climate change on the carbonation in concrete due to Carbon Dioxide ingress: Experimental Investigation and Modelling

Abbas S. AL-Ameeri [a,b] M. Imran Rafiq [b] , Ourania Tsioulou [b] and Oyuna Rybdylova [c]

(a) Engineering College, University of Babylon, Babylon, Iraq.
(b) School of Environment and Technology, University of Brighton, Brighton, UK.
(c) School of Computing, Engineering and Mathematics, University of Brighton, Brighton, UK.

ABSTRACT

Greenhouse gases (GHG), in terms of CO_2 emissions, cause a greenhouse impact leading to changes in the planet's temperature and relative humidity (RH). These changes in CO_2, temperature and RH (leading to changes in the internal moisture content) have considerable impacts on the depth of carbonation (DoC) in existing concrete structures. However, the models to forecast the DoC as a function of time in the cracked and uncracked concrete members are scarce and have limitations in terms of incorporating key variables relevant to the climate change. This study aims to develop an integrated deterioration model of carbonation in concrete. The combined impacts of variations in the internal factors (such as mechanical properties of concrete, porosity and crack width) and external factors (such as $\%CO_2$, %RH and temperature), on chemical reaction rates due to carbonation in concrete were considered. This model is based on simultaneous solutions of the diffusivity and reaction activites of $CO_{2(aq)}$ and $Ca(OH)_{2(aq)}$. The proposed model was validated using the accelerated carbonation experiments involving different properties of concrete and cracks widths. Finally, this model was employed to forecast the DoC in order to identify corrosion state owing to impact of climate change scenarios of the Inter-governmental Panel of Climate Change (IPCC 2014) and the UKCP'09 climate projections.

Keyword: *Carbonation, numerical model, global warming, phenolphthalein, crack width*

1. Introduction and background

Carbon dioxide (CO_2) forms the main gas of greenhouse gas emission (GHG) and due to an increase of human activities that lead to an increase in the average concentration of these gases continuously with time. Hence, greenhouse gas (GHG), in term of carbon dioxide (CO_2) is the main parameter affecting climate change, which considers a major threat to the environment. It is generally agreed that greenhouse gases (GHG) in terms of CO_2 emission is the main contributor to global warming [1]. Where GHG also controls radiation, forcing the climate system into global warming or climate change.

At the same time, the increase in average carbon dioxide (CO_2) concentration and temperature significantly affect the durability of concrete structures, particularly concerning carbonation and chloride penetration.

The latest scenario projections of the Inter-governmental panel on climate change (IPCC), Assessment Report 5 of IPCC (2014 AR-5) [2] has suggested four Representative Concentration Pathways, RCPs (lines), RCP 2.6, RCP 4.5, RCP 6.0 and RCP 8.5 of emissions of GHG, carbon dioxide (CO_2) and temperature. RCP 8.5 is the worst exception scenario of IPCC (2014); it forecasts that carbon dioxide concentration may exceed 1000 ppm and the mean increase of temperature may range between 2.8 to 5.75°C in 2100. Whereas, UKCP'09(2010) [3] considered the IPCC (2007) [4], A1F1 scenario to be the worst changes in temperature and CO_2 concentration, whereby the average concentration of CO_2 would approach 710 ppm.

Premature deterioration of concrete structures currently is a major global concern for the construction industry throughout the world [5]. Therefore, many requirements have been proposed by the codes of practice to maintain the durability of concrete structures in terms of chloride attack, carbonation, and corrosion for the construction of new buildings. The codes of practice recommendations for existing concrete structures focus on the evaluation and monitoring of these structures by non-destructive testing and proposing models to investigate and establish the deterioration in these structures to repair and rehabilitate.

Several models have been proposed to simulate the DoC in concrete that is based on the properties of concrete and a given exposure condition. The CO_2 diffusivity-based models are those chemical-empirical models based mainly on Fick's laws to predict the depth of carbonation (DoC), as follows;

(i): Carbonation Depth in Concrete Based on Fick's First Law

Carbonation in concrete is dependent mainly upon the availability of CO_2 and water to form CO_3^{2-}. The speed of carbonation depends on how the CO_2 and /or the CO_3^{2-} can penetrate the concrete and react with cement hydration products. The users of Fick's First law assumes a constant supply of CO_2 and that the diffusion through the surface of the concrete is constant over time. In this case, diffusion is the mass transportation of CO_2 down a concentration gradient. The diffusion of CO_2 and /or the CO_3^{2-} is based on the steady-state of diffusion of carbonate ions in porous materials as shown in Equation1 [6, 7,8,9].

$$DoC = K\sqrt{t} \qquad (1)$$

where: K (carbonation rate) ($mm/\sqrt{y}$) in time (t).

This model amalgamates all the external and internal factors, such as environmental exposure conditions, the pore structure of the concrete, the quantity of $Ca(OH)_2$ [10] and uses of supplementary

cementitious materials (SCMs) in concrete [11] into one single constant, K limiting the abilities of the model to predict for a wide range of structures in use. On the other hand, the diffusion of CO_2 or the CO_3^{2-} through the unit area of concrete is not constant or non-steady-state [12].

(ii) Carbonation Depth in Concrete Based on Fick's Second Law

The concentration of carbon dioxide in the atmosphere affects carbonation in concrete in two ways; firstly, the movement of carbon dioxide into concrete is a result of diffusion, a higher concentration gradient between the exterior and interior of concrete will lead to a greater rate of diffusion. Secondly, the higher concentration of CO_2 will yield a higher rate of reaction to form carbonation, $CaCO_3$ [12].

The diffusion and concentration of CO_2 changes both with the depth of concrete exposure to environment CO_2 and with time due to changes in the atmospheric CO_2 concentration and the amount of CO_2 consumed in carbonation. Therefore, non-steady-state of diffusion using Fick's Second Law has been the focus of attention in recent literature where the concentration of CO_2 alters with time and location factor, ∂x and ∂t respectively as shown in Equation 2. Fick's Second Law gives alteration in concentration with depth [7].

$$\frac{\partial}{\partial t}(C_{CO_2}) = D_{CO_2}\frac{\partial^2}{\partial x^2}(C_{CO_2}) \qquad (2)$$

where: the D_{CO2} is the CO_2 diffusion coefficient, C_{CO2} is the atmospheric CO_2 concentration %.

CEB-FIP (2013) and Dyer (2014) [12,13] proposed the analytical solution or modifications of Equation 2 in Equations 3 could predict the depth of carbonation (DoC) in concrete; this Equation is a function of diffusivity and concentration of carbon dioxide in concrete.

$$DoC = \sqrt{\frac{2D_{CO_2}(C_{CO_2}/100)t}{a}} \qquad (3)$$

where: D_{CO2} is the CO_2 diffusion coefficient, C_{CO2} is atmospheric CO_2 concentration %, a is the amount of CO_2 uptake to complete carbonation by assuming the 0.75 of hydrated cement could carbonate.

Talukdar *et al*. (2012)[10] have proposed a model based on a group of partial differential equations of diffusion of $CO_{2(aq)}$ and $Ca(OH)_{2(aq)}$. These are based on Fick's Second Law to find the concentration of $CO_{2(aq)}$ and $Ca(OH)_{2(aq)}$ in the depth of concrete (x) and the time (*t)* by using the solution of these equations. Talukdar *et al*. (2012)[10] assumed one-dimensional diffusion of CO_2 and $Ca(OH)_2$ to find the concentration at *x* and *t*. Their model did not utilise the minimum concentration of CO_2 and $Ca(OH)_2$ required to forms $CaCO_3$ and to establish the DoC. Talukdar *et al*. (2012) [10] assumed that the CO_2 *(aq)* is consumed by $Ca(OH)_2$ *(aq)* only, however about one half of CO_2 *(aq)* is consumed in concrete by reacting with $Ca(OH)_2$ *(aq)* and the second half of CO_2 *(aq)* is depleted by *C-S-H* [14,15]. The diffusion coefficient D_{CO2} is a variable that depends on

the microstructures of concrete (connective porosity) and microclimate condition especially the temperature and the internal moisture of the cement paste in concrete [7,10] as well as the crack in concrete samples) [16].

Equation 2 signifies that the diffusion coefficient of CO_2 is a major factor in stimulating the models to find the concentration of CO_2 in order to predict DoC. Therefore, this study aims to develop an integrated model for the diffusion coefficient and concentration of $CO_{2(aq)}$ and $Ca(OH)_{2(aq)}$ in existing concrete structures incorporating factors affected by climate parameters such as carbon dioxide concentration, temperature, and relative humidity, in addition to the properties of concrete and crack width to predict DoC. The exposure environments, CO_2, temperature, and RH, have a considerable impact on the carbonation rate of concrete structures [11]. Chi et al.(2002) [12] observed a linear correlation between the increase in the CO_2 concentration and the increase in the rate of carbonation. Drouet et al. (2019) [17] tested two hardened cement pastes using 100% CO_2 at different temperature and relative humidity (RH) and concluded that the impact of temperature on carbonation rate is dependent on the types of cement. Even though there is a chemical explanation about the temperature dependence of the diffusion coefficient based on an Arrhenius Equation [10,12,14], investigations on the effect of temperature on DoC scarce in the literature. It was also concluded that the decrease in RH to specific limites causes an increase in the carbonation depth. Where, Roy et al.(1999) [18] concluded that there is a significant increase in carbonation rate when relative humidity, RH, ranges between 52-75%. However, there is a reduction in it as the relative humidity increases by up to 84%.

This model is then used to forecast the impact of climate change on the carbonation and durability of concrete, based on the latest projection scenario, IPCC (2014)[2], since to date the published literature dealing with the impact of climate change on the durability of concrete, focused mainly on the projections of the previous scenario of the Inter-governmental Panel on Climate Change report in 2007(IPCC-2007)[4].

In summary, the increase in atmospheric CO_2 concentration is a significant factor in global warming of the environment, which causes an increase in temperature and sea level and a decrease in relative humidity. The listed information related to CO_2 concentration, temperature, relative humidity, and their changes, as well properties of concrete and crack width will be the main parameters utilized together in the research methodology of this study to find the relationship of these parameters to propose an integrated model of carbonation in concrete structures.

2. Experimental Programme

Experimental tests were conducted to quantify the effect of main parameters on the carbonation depth and for the validation of the developed carbonation model. The tests established the depth of

carbonation under different CO_2 concentration, temperature and relative humidity applying to different concrete types/ strengths. The concrete samples were cast, cured, and exposed to accelerated carbonation testing method in a University of Brighton laboratories using a CO_2 incubator. This incubator was able to automatically control temperature, CO_2 concentration, and relative humidity. Portland limestone cement (CEM II/A-LL 32,5R) with a specific gravity of 3.05 was used in this study. The chemical and physical properties of the cement comply with BS EN 197- 1: 2011 [19]. Natural sand was used as fine aggregate (particle size < 5mm), and the coarse aggregate used was crushed gravel with the size ranging from 5-14 mm. The grain size distribution, and maximum chloride and sulphate content within the aggregates comply with BS 12620:2002+A1:2008 [20]. To achieve various properties of concrete, different water to cement ratios were used. The mix proportions (water, cement, sand and gravel) were listed in Table 1.

Table 1: Concrete mixes designs used in this study

Mix symbol	Content per unit volume of concrete (kg / m^3)				
	w/c	Cement	Water	Sand	Gravel
M 0.4	0.4	513	205	653	980
M 0.5	0.5	410	205	711	1023
M 0.6	0.6	350	205	711	1041

100*100*500 mm reinforced concrete prisms and 100 mm cubes were cast in two layers, demoulded and cured in a sink filled up with tap water for 28 days. The carbonation prisms were stored in a lab environment condition (25 °C, 60% RH) for some time to dry and achieve a uniform moisture profile at the concrete surface. In this study, four different crack width ranges, (0, 0.05-0.15mm, 0.15-0.25mm and 0.25-0.35mm) were applied to concrete prisms. The flexural method was employed to induce the cracks, reinforced concrete prisms were used by fixing reinforcement in moulds with concrete cover 2 cm to control the crack width in concrete prisms. The one face of the specimens was exposed to accelerated environment conditions in a CO_2 incubator under the different exposure scenarios.

Compressive strength and porosity were also determined for all mixes. The porosity and compressive strength tests were performed in accordance with ASTM C642:2013[21] and BS EN 12390-3:2000[22] respectively by using 100 mm cube specimens. The test method given in BS EN 12390-10:2007[23] was used to determine the depth of carbonation (DoC) using phenolphthalein

solution prepared with one gram of phenolphthalein powder and dissolved into a solution of 70 ml and 30 ml of ethanol and deionized water respectively.

Three CO_2 concentration (1.5%, 3% and 5%), three relative humidity level (65, 75 and 85) and three temperature degree (25, 35 and 45) have been chosen for the experimental work, each exposure scenario lasting 8 weeks duration at the concrete age 30 days. The CO_2 concentration used in experimental works is within concentration that makes the same mineral change in concrete due to carbonation at atmospheric CO_2 concentration [24]. The experimental programme and various exposure scenarios are outlined in Table 2. For each type of mix, and each crack width case and each series, twelve specimens of concrete were prepared. This provides the results from a total of 252 prisms for this study.

After eight weeks of exposure, the prisms were taken out of the *CO_2* incubator, and the cracked area of the prisms (250 mm length) were separated using a dry saw-cut. These were then split into two half (using the compression machine) and sprayed with the phenolphthalein indicator to measure DoC (BS EN 12390-10:2007)[23]. For the uncracked regions, the DoC (which is the depth of the colourless region, X_p, after phenolphthalein spray (pH < 9)) was measured at three points perpendicular to the exposed face immediately after spraying the indicator and the average value of the DoC is reported in the results section. Whereas for the cracked regions, the DoC was measured at the location of the crack tip (as the depth of the colourless region perpendicular to the exposed face (see Figure 1-b)). A typical image of the cracked and uncracked sample split face after the phenolphthalein spray is illustrated in Figure1.

Table 2: Scenario of environmental exposure conditions of the experimental programme

Scenarios	Series No.	Environmental exposure condition			Duration of exposure (weeks)
		CO_2 (%)	Temperature (°C)	Humidity (%)	
Scenario a	7	1.5	25	65	8
	6	3	25	65	8
	5	5	25	65	8
Scenario b	5	5	25	65	8
	3	5	35	65	8
	1	5	45	65	8
Scenario c	5	5	25	65	8
	4	5	25	75	8
	2	5	25	85	8

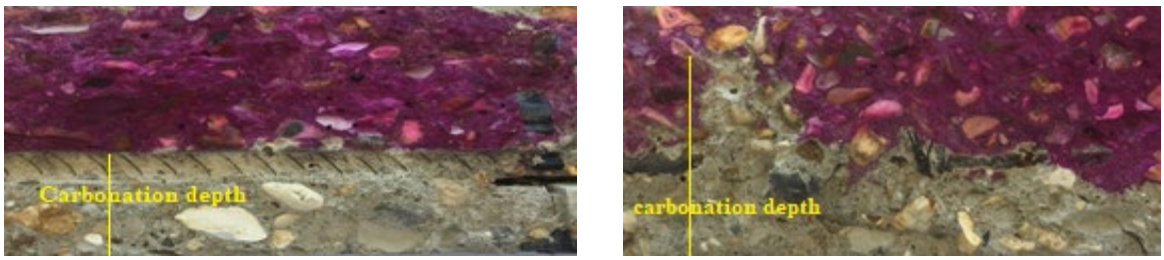

a: uncracked region b: cracked region

Figure 1: DoC (X_p,colourless phenolphthalein depth) at (a) uncracked and (b) cracked sample

3. Model development and verification

3.1 Carbonation reactions in concrete

Carbonation is the chemical reaction between carbonic acid (H_2CO_3), resulting from a combination of atmospheric carbon dioxide (CO_2) with water, and calcium ion (Ca^{2+}) from the dissolution of hydrated cement products such as calcium hydroxyl $Ca(OH)_2$, calcium silicate hydrates (C-S-H) and calcium aluminates hydrates (C-A-H). The CO_2 is consumed in two steps within the carbonation process. Initially, CO_2 is consumed by the $Ca(OH)_2$ within the concrete leading to its depletion. This is followed by the consumption of CO_2 by the C-S-H and C-A-S to densify the microstructure of cement products [15,25]. Park (2008) [15] has suggested about half of the CO_2 is consumed in each of these steps. The reactions leading to the formation of calcium carbonate ($CaCO_3$) are shown in Equations. 4 to 7 [9,26].

$$CO_2(gas) + H_2O = H_2CO_3(aq) \quad (4)$$

$$Ca(OH)_2 + H_2CO_3(aq) = Ca_2CO_3 + H_2O \quad (5)$$

$$3CaO.2SiO_2.3H_2O + 3H_2CO_3(aq) = 3CaCO_3 + 2SiO_2 + 3H_2O \quad (6)$$

$$4CaO.Al_2O_3.13H_2O + 3H_2CO_3(aq) = 4CaCO_3 + 2Al(OH)_3 + 10H_2O \quad (7)$$

3.2 FrameWork for Model development

The proposed method of estimating carbonation depth relies upon a numerical model involving the simultaneous solution of equations for the diffusivity of $CO_{2(aq)}$ and the reaction of $Ca(OH)_{2(aq)}$ in concrete specimens [15] as shown in Figure 2 and Equation8-9. One-dimensional diffusion of $CO_{2(aq)}$ into concrete sample should be simulated assuming non-steady-state diffusion by Fick's Second Law.

$$\frac{\partial}{\partial t}[CO_{2(aq)}] = D_{CO_2}\frac{\partial^2}{\partial x^2}[CO_{2(aq)}] - \frac{k_c}{2}[CO_{2(aq)}][Ca(OH)_{2(aq)}] \quad (8)$$

$$\frac{\partial}{\partial t}[Ca(OH)_{2(aq)}] = D_{Ca(OH)_2}\frac{\partial^2}{\partial x^2}[Ca(OH)_{2(aq)}] - \frac{k_c}{2}[CO_{2(aq)}][Ca(OH)_{2(aq)}] \quad (9)$$

where: $CO_{2(aq)}$, $Ca(OH)_{2(aq)}$ are Aqueous concentration of *CO_2 and $Ca(OH)_2$* respectively, *k_c is* the rate constant of reaction *x* is the depth of concrete and time *t.*

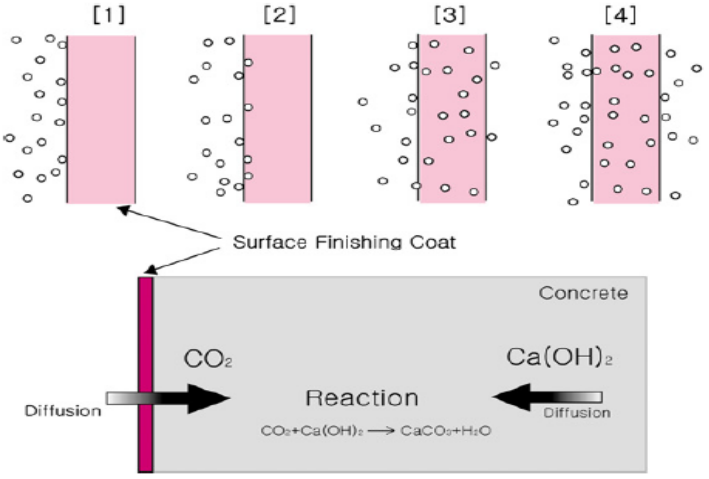

Figure 2: Mechanism of diffusion of carbon dioxide and concrete carbonation [15]

The numerical analysis of ($CO_{2(aq)}$ and $[Ca(OH)_{2(aq)}]$) diffusivity is a function of concrete properties and exposure conditions; some properties were obtained from experimental results such as density, porosity and compressive strength (see Table A.1). While, others were calculated such as the carbon dioxide diffusion coefficient, whilst the modulus of elasticity and Poisson's ratio was based on the proposed equations by AL-Ameeri *et al*. (2013) and AL-Ameeri and AL-Rawi (2009) [27,287] respectively. While, the thermal conductivity, *Tc* is computed according to the relationships proposed in ACI 122R (2002) [29]. The steps of using the simulation are summarized in Figure 3.

3.3 Diffusion Coefficient of Carbon Dioxide (D_{CO2})

Essentially, the size and connectivity of the pore within the micro-structure of concrete is the main path for the diffusion of CO_2 in concrete. This porous media mainly depends on the ratio of water/cementitious materials (w/cm), and the degree of hydration of cement (Neville, 2011) [26].

Papadakis *et al*. (1991); Papadakis and Tsimas. (2002) [30,31] proposed an empirical equation to calculate the effective diffusivity of CO_2 in concrete (D_{CO_2}) based on its porosity by:

$$D_{CO_2,ref} = 6.1 * 10^{-6}\left(\frac{(w-0.267(C+kP))/1000}{\frac{C+kP}{\rho_C}+\frac{w}{\rho w}}\right)^3 \quad (10)$$

where: *C* is the cement content (kg), *w* is the water content (kg), ρ_C is the absolute density of cement (3050 - 3150 kg/m^3), ρw is the density of water (1000 kg/m^3).

The absolute density of supplementary cementing materials is not equal to the absolute density of cement, for example, the absolute density of fly ash ranges between 1900-2800 kg/m^3, while, the absolute density of cement is about 3150 kg/m^3 and it may be less than 3150 kg/m^3 if the cement contains limestone or any additive material that has a density lower than the density of cement. To account for this variability, the above equation is modified to account for these properties of the material as shown in Equation 10.

$$D_{CO_2,ref} = 6.1 * 10^{-6} \left(\frac{\frac{w-0.267(C+kP)}{\rho_w}}{\frac{C}{\rho_C} + \frac{kP}{\rho_P} + \frac{W}{\rho_w}} \right)^3 \qquad (11)$$

where: ρ_P is the absolute density of supplementary cementing materials.

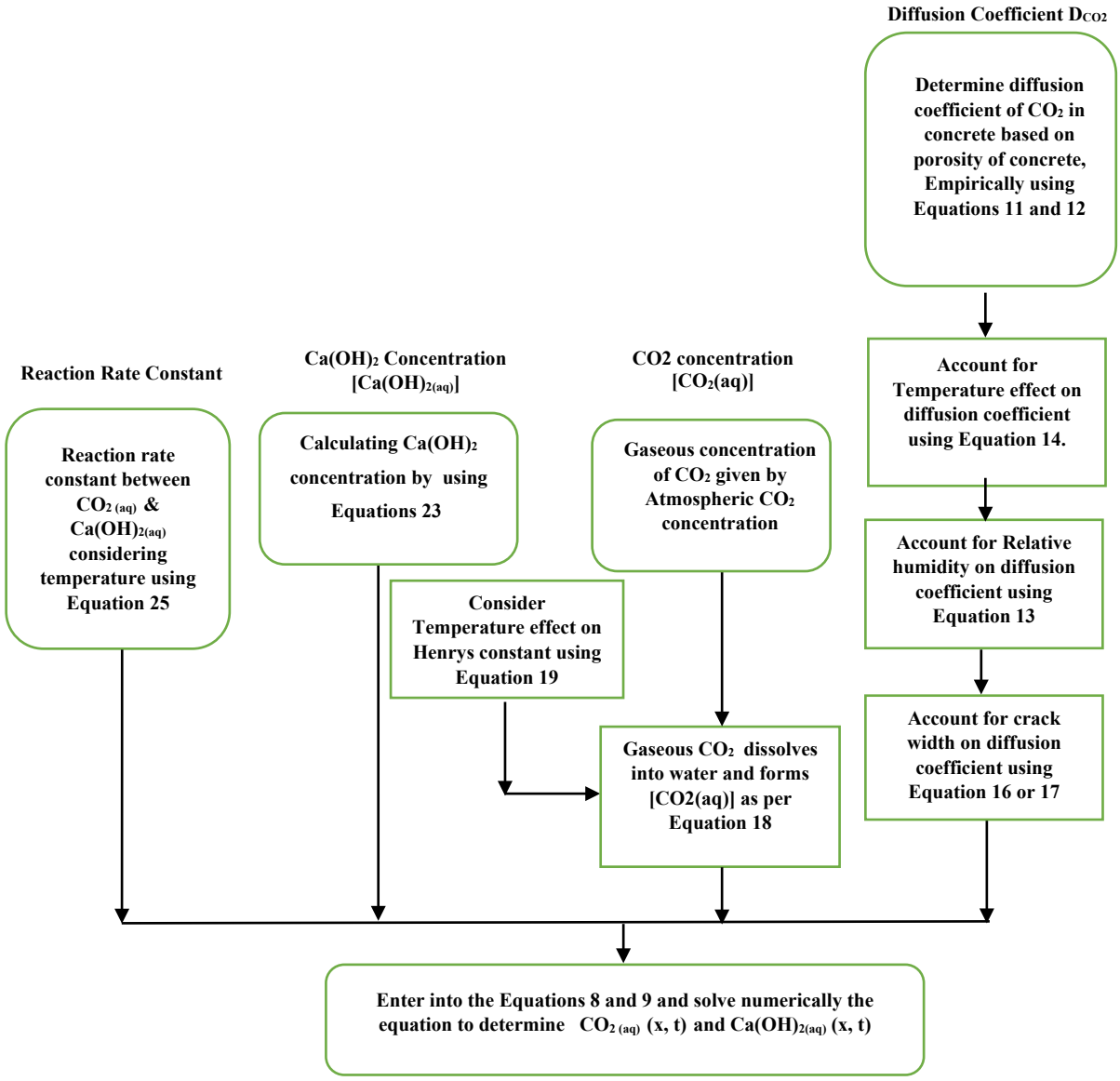

Figure 3: Flowchart to determine concentration of $CO_{2\,(aq)}$ and $Ca(OH)_{2(aq)}$

Initially, the diffusion coefficient is established for concrete under a defined climatic condition (termed as reference diffusion coefficient), which is then modified to account for the

factors related to climate change and change in material properties i.e. temperature, relative humidity and the crack width in concrete, to obtain the DoC after a defined period. Talukdar *et al.* (2012)[10] considered the effect of temperature, *T*, pore relative humidity, *RH* on D_{CO2}, but they did not consider the influence of crack and properties of concrete on the D_{CO2}. On the other hand, Kwon and Na (2011) [16] take into account the effect of crack width, W_c on the D_{CO2}, based on field investigation without consideration to the type of concrete. Because the main objective of this study is to investigate the effect of climate change on the durability of concrete structures. The study should focus on the effects of global climate change, change in CO_2 concentrations, temperature, relative humidity as well as crack width and the properties of concrete (different types of concrete) on carbonation. Therefore, these parameters, *T, RH, W* and properties of concrete will be considered in this study to account for the D_{CO2} as shown in Equation 11 and in predicting the DoC and the initiation of corrosion time, t_i due to carbonation.

$$D_{CO2} = D_{CO_2,ref} f_{C1}(T) f_{C2}(RH) f_{C3}(W_c) \quad (12)$$

where: $D_{CO2,ref}$ is the value of D_{CO2} at the reference condition (i.e. at the reference temperature, time and relative humidity) and it can be obtained by Equation 12, $f_{c1}(T), f_{c2}(RH), f_{c3}(W_c)$ are a function of temperature, relative humidity and crack width respectively, which are elaborated further in the following sections.

a. Relative Humidity Dependence on D_{CO2}

Relative humidity impacts the diffusivity of carbon dioxide into the concrete. Based on the experimental tests, Papadikas and Tsimas (2002) [31] proposed the following relationship to establish the D_{CO2} for different relative humidity:

$$f_{c2}(RH) = (1 - RH)^{2.2} \quad (13)$$

where: $f_{c2}(RH)$ is the effective factor of diffusivity of CO_2 in concrete due to relative humidity, RH is the ambient relative humidity expressed as a fraction not less than 50%.

b. Temperature Dependence on D_{CO2}

The diffusivity of CO_2 and occurring the carbonation products can be broken down into two sequences; the CO_2 dissolves into the pore water coating the pore walls and reacts with dissolved $Ca(OH)_{2(aq)}$ to form $CaCO_3(s)$ which precipitates out of the solution. The temperature of the environment of concrete can be affected by these sequences[12]. Accordingly, Talukdar *et al*. (2012); Yoon *et al*. (2007) [10,14] have employed the Arrhenius Equation (Equation 14) to account for the temperature dependence of the diffusion coefficient of CO_2 in concrete.

$$f_{c1}(T) = exp\left[\frac{U_c}{R}\left(\frac{1}{T_{ref}} - \frac{1}{T}\right)\right] \quad (14)$$

where: U_C is the diffusion activation energy, the activation energy for CO_2 diffusing in concrete has been experimentally determined as 39,000 J/mole K, R is the gas constant (8.314 J/mole. K), T_{ref} is a reference temperature (298 K) and T is the temperature of interest (K).

The experimental data on the effect of temperature from this study (see Table A.3) and from the literature, e.g. He (2010) [32] demonstrated that the results from the Arrhenius Equation overestimate the effect of temperature. Where an increased percentage in DoC due to the influence of temperature ranged from 3% to 23 % for different types of concrete and temperature. Table 3 and Figure 4 show temperature dependence factor, f_{c1}(T) values of using Arrhenius Equation and data obtained from the analysis of experimental data.

Table 3: $f_{c1}(T)$ values of applying Arrhenius Equation and values obtained by analysing experimental data

Temperature K	f_{c1}(T) obtained by applying the Arrhenius Equation	f_{c1}(T) proposed by analysing experimental data
298	1.00	1.00
308	1.67	1.17
318	2.69	1.38

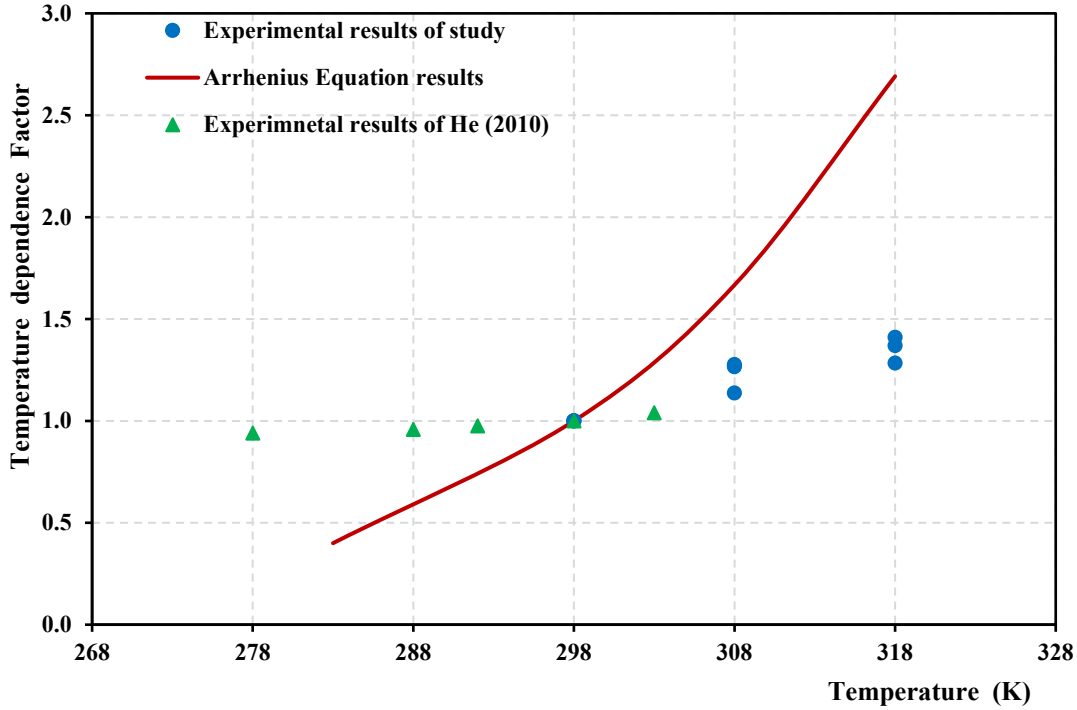

Figure 4: Temperature dependence factor for using Arrhenius Equation and experimental results of this study and He (2010)[32]

The Arrhenius Equation is modified as shown in Equation 15 using an adjustment factor, b, which is calculated from the experimental data to account for the above different using non-linear regression analysis because the Arrhenius Equation is general is used in a chemical reaction between materials with different temperature. The main data for the series exposed to temperatures 25, 35 °C and 45 °C was used in this analysis to find the temperature influence on $f_{c1(T)}$. The correlation coefficient (R) was 0.87 and all correlations were statistically significant at the P= 0.000 level confidence 95% (alpha 0.005).

$$f_{c1}(T) = exp\,[(b)\,\frac{U_c}{R}(\frac{1}{T_{ref}} - \frac{1}{T})] \qquad (15)$$

where: b is the adjustment factor (0.322).

c. Crack Dependence on D_{CO2}

The cracks in concrete have a significant impact on the penetrability of carbon dioxide. As a result, the carbonation may be faster in cracked concrete compared with un-cracked concrete [33]. Kwon and Na (2011); Smilauer *et al*. (2013) [16,34] suggested a model predict the depth of carbonation (DoC) in cracked concrete from field investigations with crack widths ranging between 0.1 mm and 0.2 mm as:

$$DoC = \left(2.816\sqrt{W_c} + 1\right)K\sqrt{t} \qquad (16)$$

where: W_c is the crack width, K is the carbonation rate in the uncracked sample.

In order to achieve crack factor $f_{c3(W)}$ (DoC $_{cracked}$/ DoC $_{uncracked}$), for a wide range of crack width W_c (0.05 to 0.35 mm), the influence of crack width on the diffusion coefficient of CO_2 (D_{CO2}) was based on the experimental data(see Table A.2, A.3 and A.4) and calculated by non-linear regression analysis (least squares) as shown in Equation 16 and Figure 5. The input data was $f_{c3(W)}$, and crack width for the cracked and non-incorporating SCMs specimens for the series exposed to 1.5-5 % CO_2 conditions. The correlation coefficient (R) was 0. 85 and all correlations were statistically significant at the P= 0.000 level and level confidence 95% (alpha 0.05) and the predicted and observed values are presented in Figure 6.

$$f_{c3(W_c)} = (11.4\sqrt{W_c} + 1) \qquad (17)$$

where: W_c is the crack width in mm and $f_{c3(W)}$ is the proportion of the diffusion coefficient of carbonation in the cracked sample ($D_{CO2(cracked)}$) to the diffusion coefficient of carbonation in the un-cracked sample ($D_{CO2(un\text{-}cracked)}$).

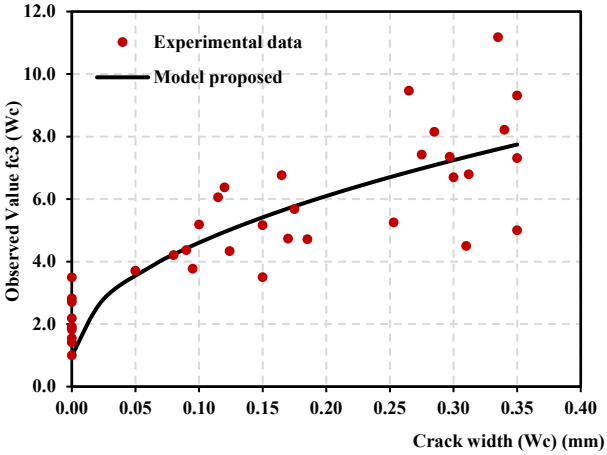

Figure 5: Effect of crack width on carbonation depth

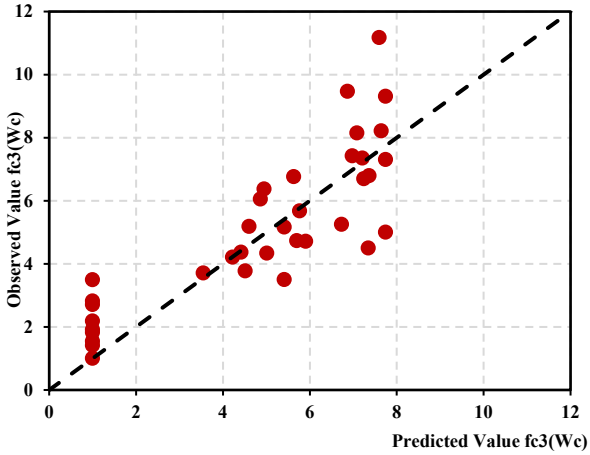

Figure 6: Observed and predicted results of the model proposed of cracked factor ($f_{c3(Wc)}$)

3.4 Numerical Formulation of Carbonation Model

Firstly, the gaseous diffusion of CO_2 is important in the carbonation of concrete and the diffusion coefficient of carbon dioxide has been described in the previous section. Upon reaching a given point in the concrete sample, the gaseous CO_2 dissolves into water and forms dissolved aqueous $CO_{2\,(aq)}$ at that location at a concentration governed by Henry's Law [14].

$$[CO_{2(aq)}] = HRTCO_{2(g)} \quad (18)$$

where: $CO_{2(g)}$ is a concentration of CO_2 as gas in an environment condition, H is the Henry's constant (mole/m^3 atm), R is the gas constant and T is the temperature (K).

Henry's constant is temperature-dependent as shown in Equation 19 [35]:

$$H(T) = H_{ref}\, exp\left[\Delta\left(\frac{1}{T_{ref}} - \frac{1}{T}\right)\right] \quad (19)$$

where: H_{ref} is the reference Henry's constant (34.2 mol/m^{3}atm) and Δ is an enthalpy constant (2400 K).

For example, the $[CO_{2(aq)}]$ was calculated and used as 1.14 M at 30 °C and 6 % $CO_{2(g)}$.

Secondly, the dissolved aqueous $Ca(OH)_{2(aq)}$ concentration in the solution of concrete depends on the degree of hydration, cement content and cement compounds, C_3S and C_2S [15]. The total amount of $Ca(OH)_2$ in the solid phase of cementation composite is calculated from the chemical composition of the hydration of cement compounds, C_3S, and C_2S as shown in Equations [26,36]:

$$2C_3S + 6H \rightarrow C_3S_2H_3 + 3CH \quad (20)$$

$$2C_2S + 4H \rightarrow C_3S_2H_3 + CH \quad (21)$$

where: C_3S is Tricalcium silicate and its molar weight (228 g/mole), C_2S is Dicalcium silicate and its molar weight (172 g/mol) and CH is calcium hydroxide and its molar weight (74 g/mole).

Then;

$$C_{CH} = \frac{M_{CH}}{2*M_{C_2S}} * C_{C_2S} + \frac{3M_{CH}}{2*M_{C_3S}} * C_{C_3S} \quad (22)$$

where: C_{CH} is $Ca(OH)_2$ content, M_{CH}, M_{C_2S} and M_{C_3S} are the molecular weight of $Ca(OH)_2$, C_2S and C_3S respectively, C_{C_2S} and C_{C_3S} are C_2S and C_3S percentage by weight of cement respectively.

Hence, the concentration of $Ca(OH)_2$ can be determined by cement content and degree of cement hydration using:

$$[Ca(OH)_2] = \frac{C_{CH}*C*\propto}{M_{CH}} \quad (23)$$

where: $[Ca(OH)_2]$ is $Ca(OH)_2$ concentration in mole/m^3 , M_{CH} is the molecular weight of $Ca(OH)_2$(74 g/mole), C is the weight of cement in m^3 and $\propto$ is hydration degree.

For the cement used in this study, the C_2S and C_3S percentages were 15.36% and 55% by weight of cement respectively and taking the hydration of cement as 90% [36], the [$Ca(OH)_2$] will become:

$$[Ca(OH)_2] = 3.685\ C \quad (24)$$

For example, [$Ca(OH)_2$] calculated for cement content mix 380 kg / m^3 is 1400 mol/m^3 (1.4 M).

The diffusion coefficient of $Ca(OH)_2$ was taken as $1*10^{-12}$ m^2/s in the analysis of diffusivity of calcium hydroxide [30]. Where Park (2008)[15] confirmed that the diffusion coefficient of $Ca(OH)_2$ may be kept at $1*10^{-12}$ m^2/s and the rate of reaction may be increased a thousandfold with a slight change in the depth of carbonation.

Thirdly, it is also significant to find the rate of reaction between $CO_{2(aq)}$ with $Ca(OH)_{2(aq)}$ to form $CaCO_3$, as this is also temperature-dependent. Khunthongkeaw and Tangtermsirikul (2005) [37] proposed a second-order relationship with a rate constant of reaction:

$$k_C = A\ e^{\frac{-U}{RT}} \quad (25)$$

where: k_c is the reaction rate constant for the reaction between $CO_{2(aq)}$ with $Ca(OH)_{2(aq)}$ at the temperature of interest (m^3/mol/s), U is the reaction activation energy (40,000 J/mol K) and A is the pre-exponential factor (1390 m^3/mol/s).

Fourthly, the domain, the initial and the boundary condition of Eqs 26 to 33 are:

$$CO_{2(g)}(x,t) \quad 0 \le x \le L \ and \ 0 \le t \le \infty \quad (26)$$

$$CO_{2(g)}(x,0) = 0 \quad for\ x > 0 \quad (27)$$

$$CO_{2(g)}(0,t) = CO_{2(g)}(atm) \quad for\ t > 0 \tag{28}$$

$$\frac{d}{dx}CO_{2(g)}(L,t) = 0 \quad zero - flux\ boundary \tag{29}$$

$$Ca(OH)_{2(g)}(x,t) \quad 0 \le x \le L\ and\ 0 \le t \le \infty \tag{30}$$

$$Ca(OH)_{2(g)}(x,0) = Ca(OH)_{2(aq)i} \quad for\ x > 0 \tag{31}$$

$$\frac{d}{dx}Ca(OH)_{2(aq)}(0,t) = 0 \quad zero - flux\ boundary \tag{32}$$

$$\frac{d}{dx}Ca(OH)_{2(aq)}(L,t) = 0 \quad zero - flux\ boundary \tag{33}$$

where: L is the thickness of the concrete sample

For concrete, the thermal diffusivity is much greater than the mass diffusivity. Therefore, the temperature of the concrete is assumed uniform at any time so that there is no need to also solve the energy equation or to account for the heat of the reaction [10]. A flowchart to demonstrate how Equation 7 and 8 are formulated is shown in Figure 3 and 7.

3.5 Frame Work of Numerical Analysis of Species Diffusion

The finite element methods have become a commonly used method in the engineering field. The finite element method, FEM, is based on dividing a structure into a number of finite elements connected by nodes [38]. In the present study, a non-linear finite element technique (NLFET) was used to determine the depth of carbonation by finding the diffusivity of $CO_{2(aq)}$ and $Ca(OH)_{2(aq)}$ in concrete using the FEM package Multiphysics. In this case, the FEM, Transport of Diluted Species in Porous Media Method (tds) was used.

3.5.1 Theory of the Transport of Species ($CO_{2(aq)}$ and $Ca(OH)_{2(aq)}$)

The transportation of diluted species interface offers a predefined exhibiting environment for studying the evolution of chemical species transported by diffusion and convection. The interface assumes that all species are dilute; which means that their concentration is small compared to a solvent fluid or solid. As a rule of thumb, a mixture containing several species can be considered diluted when the concentration of the solvent is more than 90 moles %. Due to the dilution, mixture properties such as density and viscosity can be assumed to correspond to those of the solvent. Fick's law governs the diffusion of the solute's dilute mixtures or solutions [12, 14]. The transportation of diluted species interface supports the simulation of chemical species transport by convection and diffusion in one dimensional (1D), two dimensions (2D), three dimensions (3D) as

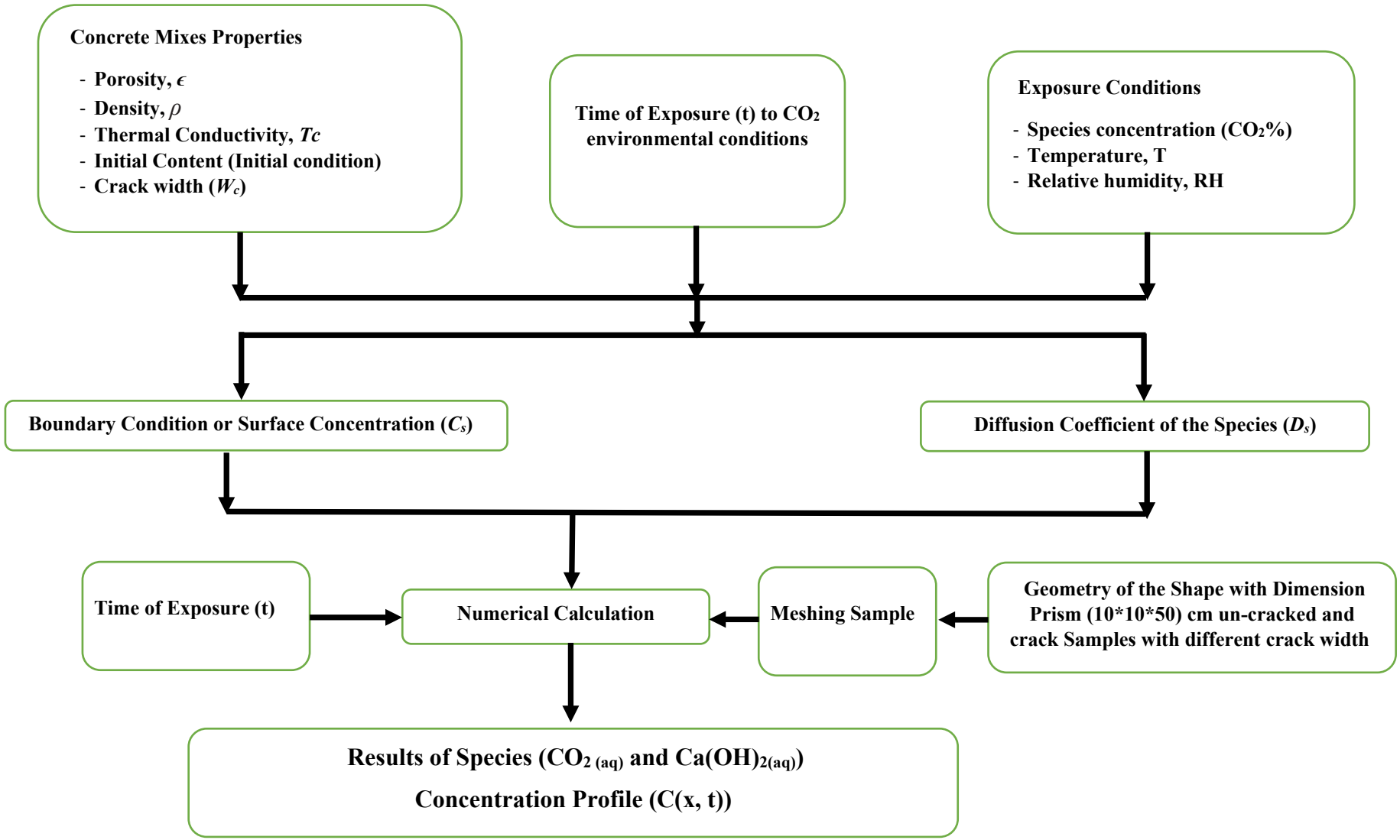

Figure 7: Flowchart of numerical analysis using the FEA programme

well as for axisymmetric models by, (i) Mass Balance Equation. (ii) Convective Term Formulation, (iii) Solving Diffusion Equation Only

3.5.2 Model Geometry and Meshing using Programme

The geometry of the full specimen was characterised by a two-dimensional full specimen (100*100*500 mm). The mesh settings determine the resolution of the finite element mesh used to discretize the model. The finite element technique is the method to divide the model into small elements of geometrically simple shapes.

Figure 8 demonstrates the simple schematic of the mesh model geometry of concrete samples (with and without a crack) which were modelled to simulate this model. The concrete was modelled with a 3-node free triangle element available in the programme's element library. This element type has concentrated integration stiffness [39]. This element can be also used for nonlinear analysis counting that of integration. The maximum and minimum element size of the mesh, and the curvature factor was 1.3 mm, 0.004 mm and 0.6 respectively.

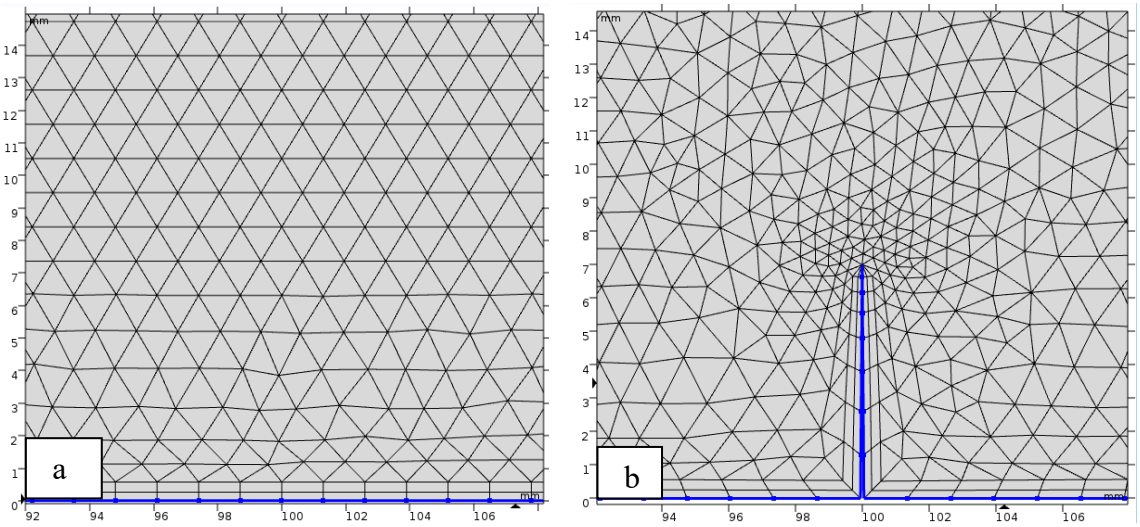

Figure 8: Geometry of meshing, (a) Un-cracked sample, (b) Cracked sample

3.5.3 Numerical Analysis of Species Diffusion of $CO_{2\,(aq)}$ and $Ca(OH)_{2(aq)}$

To simplify the analysis, a numerical analysis was used to solve these equations simultaneously and determine the concentrations of $CO_{2\,(aq)}$ and $Ca(OH)_{2(aq)}$ at a given location and time within the concrete specimen due to exposure to CO_2 environment as shown in Figure 9. The simulation of the concentration of $CO_{2\,(aq)}$ and $Ca(OH)_{2(aq)}$ profile is presented in Figure 10 and 11 respectively for example in the results test of Talukdar *et al.* (2012)[10].

The results illustrate the concentration of $CO_2(_{aq})$ reduces with depth due to the decrease of $CO_2(_{aq})$ diffusivity into the concrete depth. Whilst, the concentration $Ca(OH)_2(_{aq})$ raises with depth due

to a decrease of consumption of $Ca(OH)_{2(aq)}$ into the concrete depth owing to reduced formation of calcium carbonate.

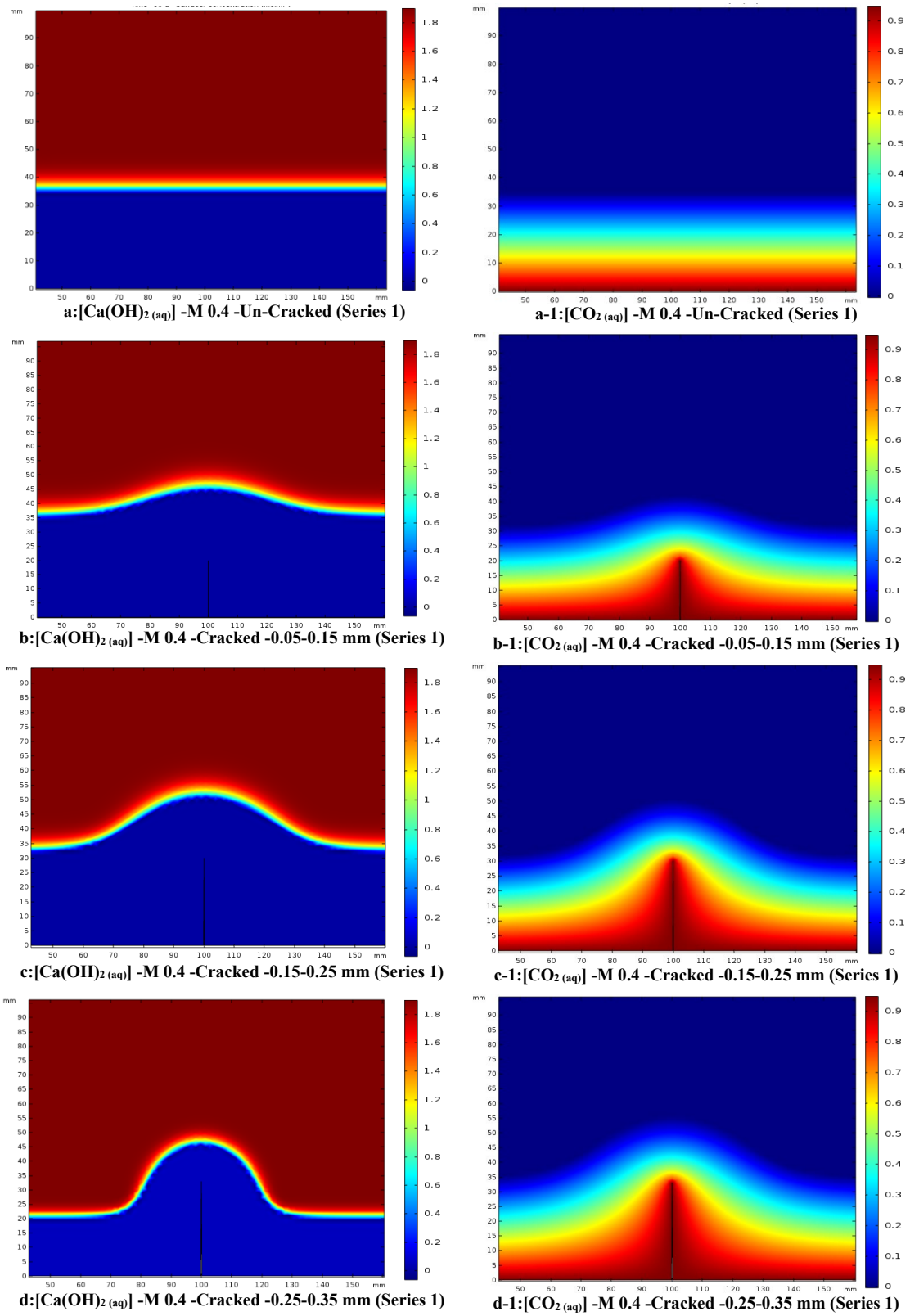

Figure 9:[$CO_{2\,(aq)}$] and [$Ca(OH)_{2\,(aq)}$] concentration distribution in the samples (cracked and uncracked) due to exposure to 5% CO_2 , 45 ºC and 65% RH for 8 weeks

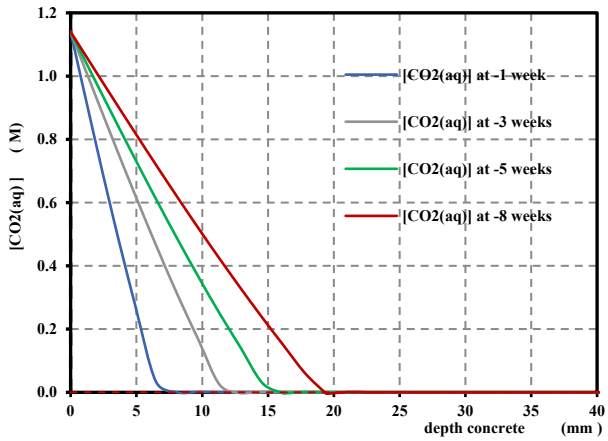

Figure 10: $CO_{2(aq)}$ concentration profile in concrete sample for 6% $CO_{2\,(g)}$,

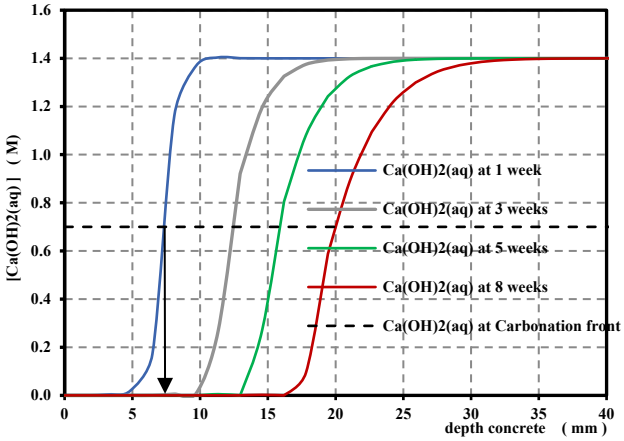

Figure 11: $Ca(OH)_{2(aq)}$ concentration profile in concrete sample for 380 kg cement content

Finally, the depth of carbonation, DoC can be determined using two assumptions:

- Park (2008) [15] found the pH of concrete drops to 9 at 50% consumption of $Ca(OH)_2$ in the concrete mixes. Therefore, Park (2008) [15] assumed the location of the carbonation front, X_f by modelling to find the location where 50% of the $Ca(OH)_2$ is consumed. The depth of carbonation front X_f relates to the depth beyond which concrete is yet unaffected by the carbonation. Then, the depth of carbonation, DoC is half of the carbonation front depth, X_f [40].

- Ehrlich *et al*. (2015) [41] reported that $CaCO_3$ will precipitate in an aqueous solution containing $10^{-4.16}$ M of $Ca(OH)_2$ when the concentration of $CO_{2(aq)}$ exceeds $10^{-4.16}$. This is because the product of the concentration of two ions of ($CO_{2(aq)}$ and $Ca(OH)_{2(aq)}$) could exceed the solubility constant (K_{sol}) for $CaCO_3$, $10^{-8.32}$. Therefore, the minimum concentration of CO_2(aq) to form the $CaCO_3$ (carbonation components) should be equal to, or more than, $10^{-4.16}$ ($6.92*10^{-5}$ M). Then, the carbonation depth at this point of concentration $10^{-4.16}$ M $CO_{2(aq)}$; beyond this depth, the concentration of $CO_{2(aq)}$ is less and $CaCO_3$ will not precipitate.

Using the above two assumptions, the depth of carbonation, DoC for experimental results are simulated and verified in the next section.

4. Verification of Numerical Modelling for the Carbonation Depth

The model is validated by comparing its results with the available experimental results of this study and other studies in the literature. The $CO_{2(aq)}$ and $Ca(OH)_{2(aq)}$ transportation and reaction in the uncracked and cracked concrete shown in Figure 12 are used in the simulation to find the DoC. The CO_2 diffusion coefficient for the samples are computed using Eqs 9-16 and is presented in Tables 4.

Predicted data for the DoC obtained through the model is compared with the respective experimental results scenarios and are presented in Figure 12.

Table 4: D_{CO2} values with pores volume ratio, temperature, relative humidity, and crack width

	Sample	C_{CO2} %	f_{c2}(RH)	f_{c1}(T)	D_{CO2} m^2/sec $*10^{-8}$			
					Un-cracked	0.05-0.15 mm	0.15-0.25 mm	0.25-0.35 mm
Series 1	M 0.4	5	0.099	1.38	0.51	3.73	5.06	6.08
	M 0.5	5	0.099	1.38	1.87	13.71	18.61	22.37
	M 0.6	5	0.099	1.38	3.56	26.08	35.41	42.57
Series 7	M 0.4	1.5	0.099	1	0.37	2.71	3.68	4.42
	M 0.5	1.5	0.099	1	1.36	9.97	13.53	16.27
	M 0.6	1.5	0.099	1	2.59	18.97	25.76	30.96

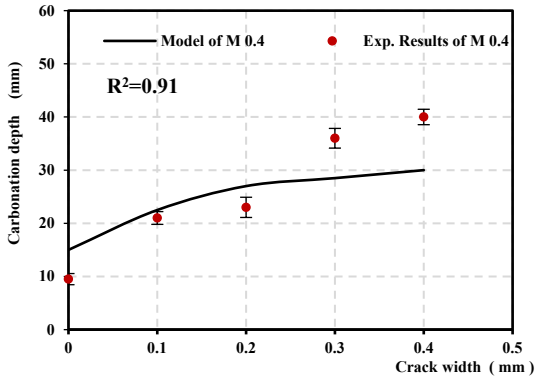

a:M 0.4 - (Series 1- 45 ºC, 65% RH and 5 CO_2)

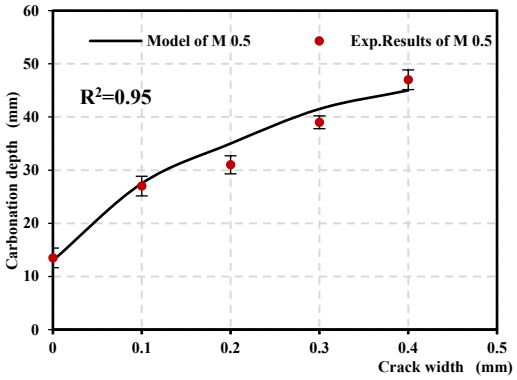

b:M 0.5 - (Series 1- 45 ºC, 65% RH and 5 CO_2)

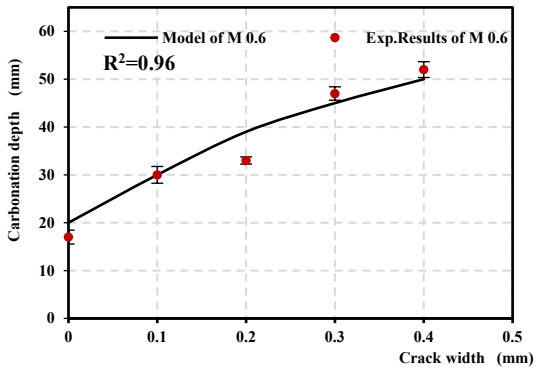

c:M 0.6 - (Series 1- 45 ºC, 65% RH and 5 CO_2)

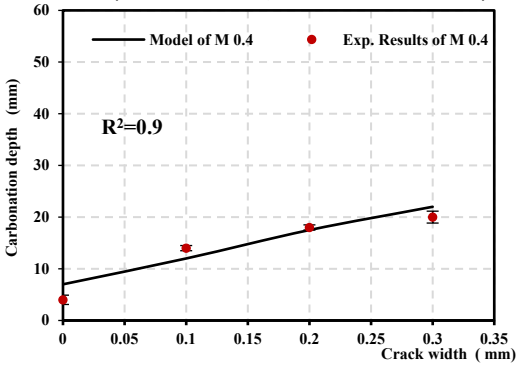

d:M 0.4 -(Series 7-25 ºC, 65% RH and 1.5 CO_2)

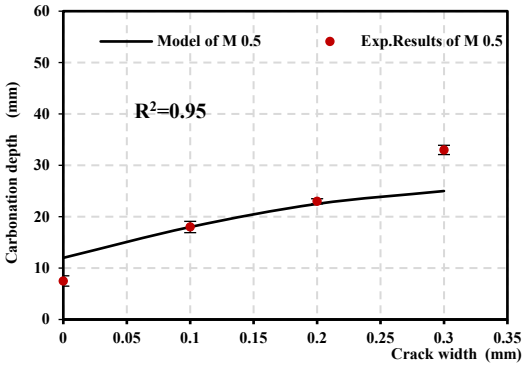

e:M 0.5 - (Series 7-25 ºC, 65% RH and 1.5 CO_2)

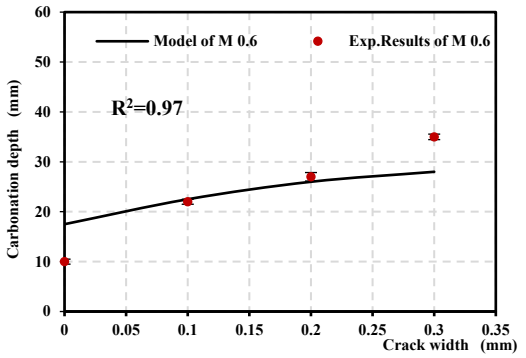

f:M 0.6 - (Series 7-25 oC, 65% RH and 1.5 CO2)

Figure 12: Carbonation depth of Numerical vs experimental results for Series 1and Series 7

The influence of properties of concrete, the crack width, % RH, CO_2 concentration and temperature were considered in the model in Equations 8 to 9 and verified by experimental results in this study as shown in Figures 12 (a-f). The predicted data of carbonation depth in cracked samples demonstrate that an increase in the crack width and depth increases the penetration and reaction of $CO_{2(aq)}$ with $Ca(OH)_2$ to precipitate $CaCO_3$.

It can be seen from Figure 12, the predicted data resulting from modelling matches well with the experimental data (the R^2 values of most of these graphs were more than 0.9). The curve fitting is less favourable in these cases; however, the trends are still correct even here. Overall, this model can be used to forecast the carbonation depth for different crack widths in concrete and different scenarios of exposure conditions (e.g. CO_2, temperature and relative humidity).

Secondly, the modelling results are verified using other studies from the literature. (Talukdar *et al*., 2012) [10] used three concrete cube specimens (10×10×10 cm) cast using OPC. The w/cm ratio and aggregate to cementitious materials (A/cm) were 50% and 4.3 respectively. After 28 days of curing, the specimens were exposed to 6% CO_2, 65% RH and 30 °C for 8 weeks. The computational results showed $f_{c2(RH)} = 0.099$, $f_{c1(T)} = 1.1$ and $D_{CO2} = 1.5*10^{-8}$ m^2/sec, and the calculation of this case compared with experimental results are presented in Figure 14-a. (Chi *et al*., 2002) [42] used three cube concrete specimens (10×10×10 cm) cast using ordinary Portland cement. The w/cm was 48%. After 28 days of curing, the specimens were exposed to 5% CO_2, 55% RH and 30°C for 8 weeks. The computational results showed $f_{c2(RH)} = 0.133$, $f_{c1(T)} = 1.1$ and $D_{CO2} = 1.6*10^{-8}$ m^2/sec, and the calculation of this case compared with experimental results are presented in Figure 14-b. The carbonation depth was measured using the phenolphthalein technique in both cases. Both cases were used to verify the numerical modelling. The predicted data and experimental results for both cases are presented in Figures 13.

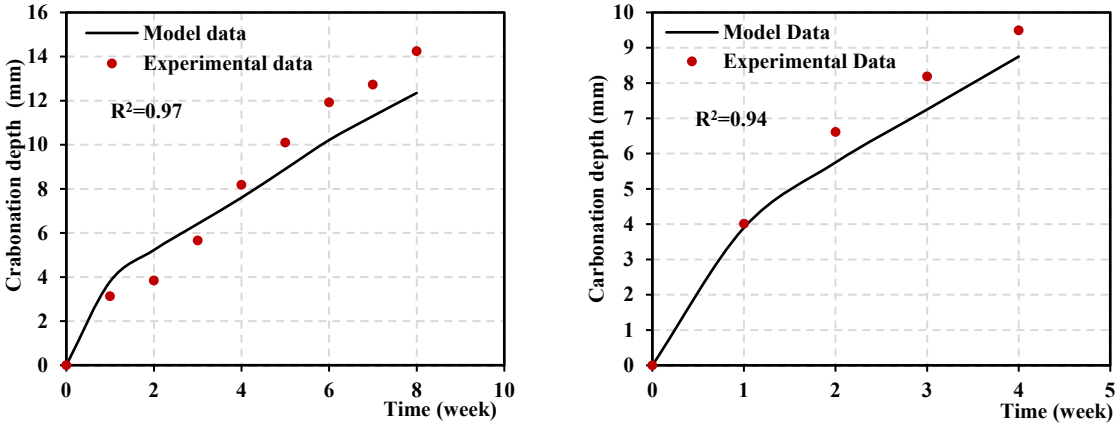

a: Talukdar *et al.* (2012) **b: Chi *et al.*(2002)**

Figure 13: Carbonation depth of Numerical vs experimental results for (a)Talukdar *et al*. (2012) [10] and (b) Chi *et al*. (2002) [42]

From Figure 13, there is a qualitative difference in trend between the experimental results and those predicted by the model as shown in R^2 values. The analytical data obtained by employing the model illustrated that the shape of the carbonation depth profile matched well (regression factor, R^2 =0.94) with the literature results. The difference between the analytical results and experimental data may be the model assumptions of reaction for $CO_{2(aq)}$ and $Ca(OH)_{2(aq)}$ or in the factors that affect carbon dioxide coefficient such as relative humidity factor. On the other hands, the experimental results are based on the change in the colour of carbonated concrete which has a pH ≤ 9 investigating by the phenolphthalein alkalinity indicator. This method of investigating carbonation only determines the full carbonated zone [42,43].

Overall, this model can be used to predict DoC in existing concrete structure with future global warming or climate change scenarios.

5. Prediction of DoC in Concrete Structure due to Climate Change using Proposed Model

As mentioned previously, climate changes affect the CO_2, T, and RH, which in turn changes the carbonation depth within concrete. The atmospheric temperature and carbon dioxide concentrations of IPCC(2014), as shown in Figure 14, will be used in this study to forecast the change in carbonation depth numerically.

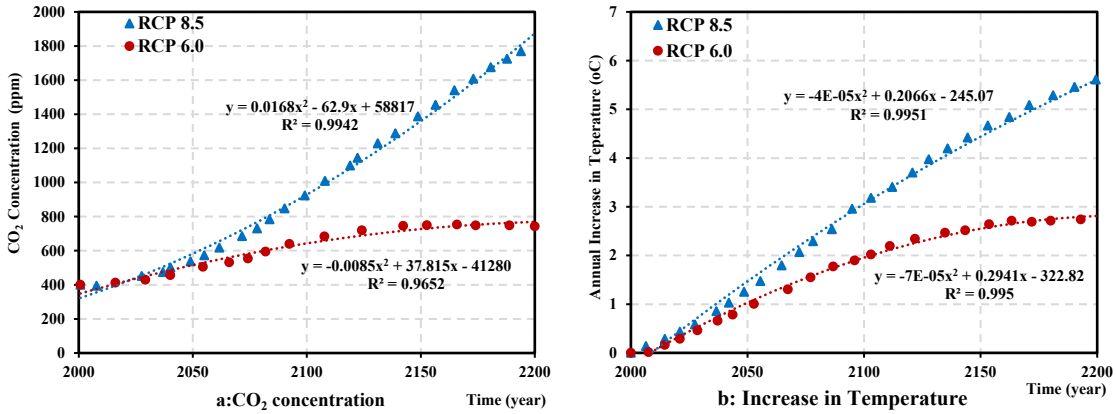

Figure 14: Prediction of atmospheric CO_2 % and progress in temperature over the period 2000-2200 for scenarios, RCP 8.5 and RCP 6.0 in (IPCC, 2014- AR5)[2]

The city of London was selected, and carbonation progression depth for a hypothetical concrete structure, having w/cm ratios, 0.4, 0.5 and 0.6 and properties of these mixes as shown in previous sections, were modelled. Based on the data of temperature and relative humidity of London - UK in the ten years from the beginning of this study, 2004-2014 which are supplied by Met Office- UK, were considered in the initial environmental exposure conditions in prediction first. Secondly, in Assessment Report –Working Group III in Emission Scenarios (IPCC, 2014- AR5,WGIII)[2], two emission scenarios were considered, the worst-case scenario (RCP 8.5), case scenario (RCP 6.0), and the control scenario (CO_2 levels held constant at initial levels of 400 ppm). Corresponding to the forecast of mean global temperature increases are obtained by data reported in the (IPCC, 2014- AR5) [2] as shown in Figure 15. A simplified climate model was employed which allowed for the development of equations for emissions, temperature, and humidity over the next 100 years for the city of London.

The numerical carbonation model to predict the DoC, considering for the first time, time-varying concentrations of CO_2, temperature, and humidity. This model was used to determine the carbonation in the case of no climate change effects (CO_2, T, and RH) and the other cases with the effect of change in (CO_2, T, and RH) due to climate change depending on time as shown in Figure14. The concrete members, having different w/cm ratios (un-cracked samples) and environmental conditions were considered to forecast the DoC up to 100 years due to exposure conditions for the three scenarios. Assuming the building goes into service in the year 2000, the carbonation depths for each mix for the three scenarios are presented in Figure 15 (a-c). On the other hand, changes in climate change parameters for different crack widths for two scenarios were considered for the carbonation depth as shown in Figure 16.

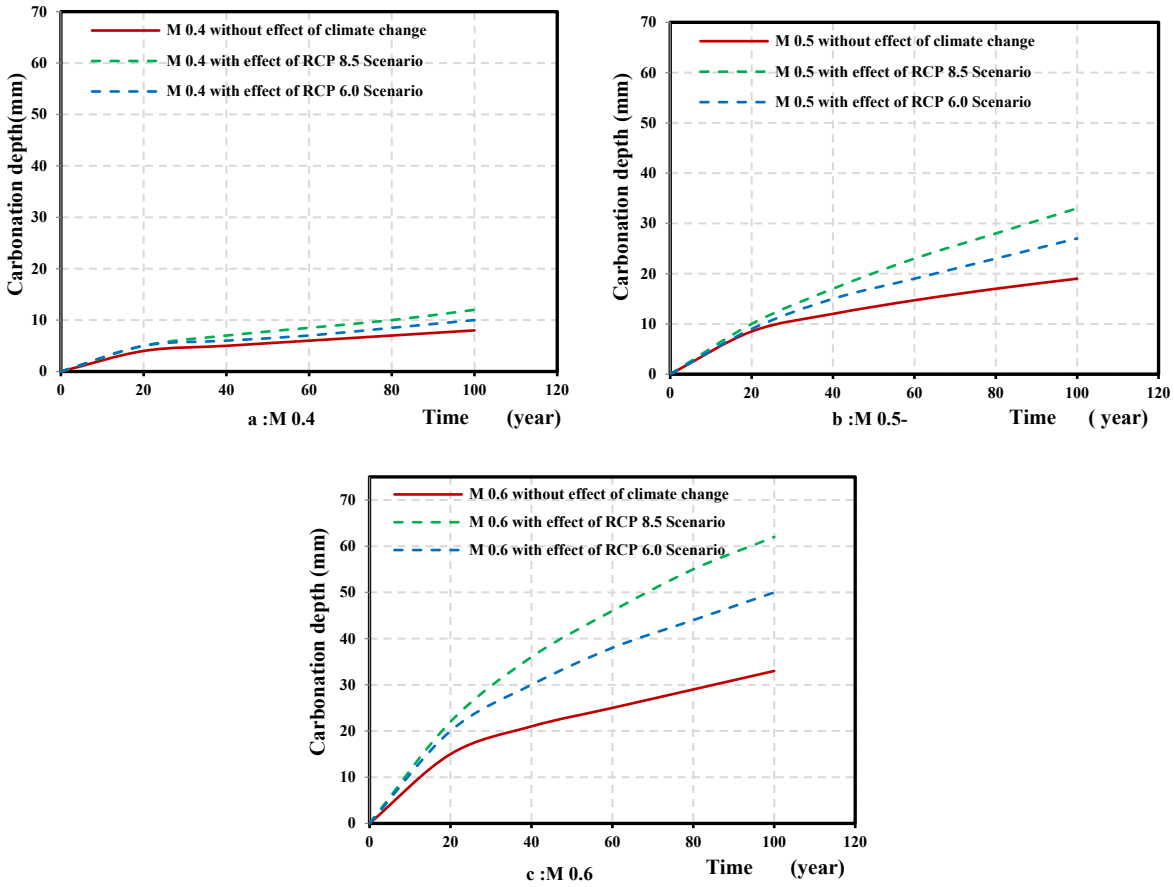

Figure 15: Effect of climate change scenarios on the prediction of carbonation depth for an un-cracked member in the city of London

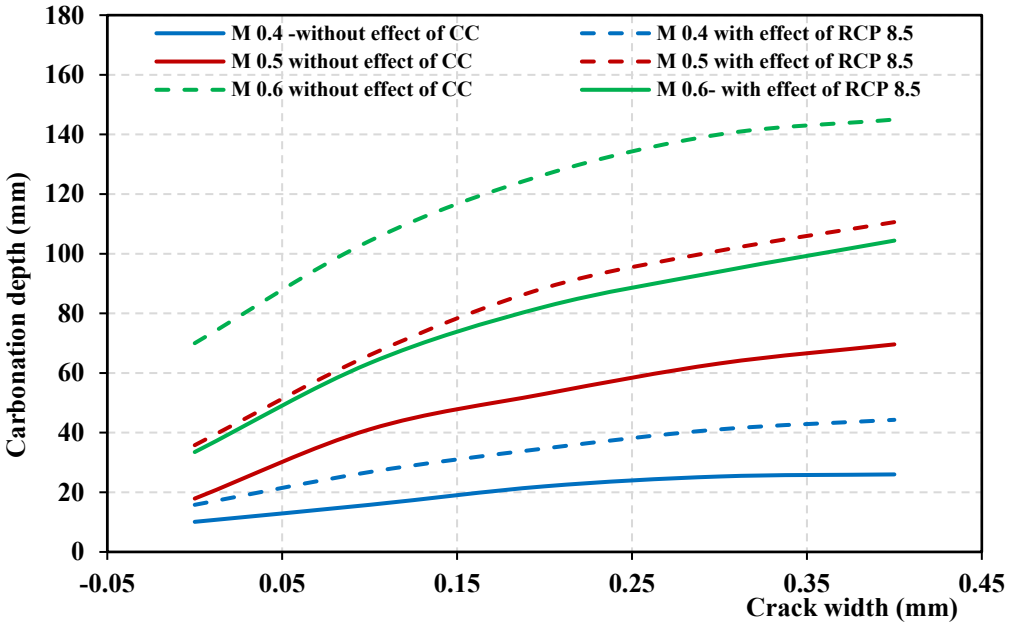

Figure 16: Effect of crack width and climate change for (RCP 8.5) on the carbonation depth of structures in the city of London in the Year 2100

From these figures, some of the observations are made.

(i): The analytical results of carbonation depth in concrete members exposed to CO_2 environment condition due to the influence of climate change parameters for IPCC (2014) models

(RCP 8.5 and RCP 6.0 scenarios) increased with the increase in CO_2, temperature and reduction humidity for both exposure condition scenarios. The percentage increase in the ultimate carbonation depths comparing the control condition for the two scenarios is listed in Table 5. While, the percentages increase in carbonation depth for the cracked concrete members (different crack widths and w/cm ratios) due to exposure condition scenario, RCP 8.5 was 63%,69% and 63% for M 0.4, M 0.5 and M 0.6 respectively.

Table 5: Effect of climate change scenarios RCP 8.5 and RCP 6.0 on carbonation progress in concrete members in the city of London

Mix designation	Scenario	Percentage increase in the ultimate carbonation depth (mm) at				
		2020	2040	2060	2080	2100
M 0.4	RCP 8.5	25	40	42	43	50
	RCP 6.0	25	20	17	21	25
M 0.5	RCP 8.5	18	42	56	65	74
	RCP 6.0	25	29	25	35	42
M 0.6	RCP 8.5	47	71	84	90	88
	RCP 6.0	33	43	52	52	52

(ii): The Carbonation progress due to the change in CO_2 and temperature is higher due to the increase of porosity of concrete (properties of concrete dependent). Carbonation progress for Mix M 0.6 with w/cm ratio 0.6 for both scenarios was higher than carbonation depths for mixes M 0.4 and M 0.5. It is seen that climate change does not begin to seriously affect the rate of carbonation until about 30 years into the future (in these simulations, the year 2030). It is only after 30 years that we start to see the carbonation depth curves for the RCP 8.5 and RCP 6.0 scenarios begin to seriously divert from the control curves for all mixes.

(iii) Finally, it is noticed that over 100 years, for these cases, there is an obvious impact of climate change on carbonation depths. However, it is also important to consider what the actual effects of climate change will be on the service life of a structure. As mentioned previously, it is observed that corrosion may occur when the distance between the carbonation depth and the reinforcement bar surface is less than 1-5 mm [14,44,45]. However, probabilistic analyses for assessing durability design specifications tend to ignore this effect [13]. Hence, the time to corrosion initiation, t_i occurs when the carbonation depth is equal to the depth of concrete cover. The times to initiation, t_i due to carbonation induced corrosion for each of the mixes (assuming the concrete cover is 25 mm) for two cases of structures in London are listed in Table 6.

Table 6: Time to corrosion initiation due to carbonation – constructed in the Year 2000

Mix designation	Scenario	Time to initiation (year)*	Ultimate carbonation Depth (mm)**
M 0.4	Control condition	> 100	8
	RCP 8.5	> 100	13
	RCP 6.0	> 100	10
M 0.5	Control condition	> 100	18
	RCP 8.5	60	33
	RCP 6.0	100	28
M 0.6	Control condition	60	34
	RCP 8.5	21	62
	RCP 6.0	24	50

*Time to initiation of corrosion is the time at the DoC ≥ 25 mm.
** Ultimate carbonation Depth is at the Year 2100.

The main factors affecting an increase in the carbonation depth is the increase of carbon dioxide concentration as well as the increase in temperature and decrease in the relative humidity. The IPCC (2014), (AR5-RCP 8.5)[2] has forecasted the change in carbon dioxide over the (21^{st}) century will reach up to double concentration by 2100 compared with 2000 that lead to an increase in the average temperature of 4.2°C as shown in Figure 14. The atmospheric carbon dioxide concentration, temperature, and humidity of the exposure environment are the main driving force for carbon dioxide penetration in concrete structures [14,46]. The model of the rate of carbonation is based on surface exposure conditions, CO_2, RH and T and properties of concrete structure [7].

Finally, considering that the structures in these cases would likely be subjected to deterioration by means other than carbonation during the same time, the reduction in initiation time caused by climate change factors would be one of many factors affecting the service life. Secondly, it is noted that there is a minimal reduction in propagation time (the difference between the time to initiation and time to failure) between the control cases, and the climate change cases, for each respective mix. Therefore, in the short term, it is reasonable to conclude that climate change will not significantly affect the durability of our concrete infrastructure. However, it was noted earlier that the effects of climate change become significant after approximately 30 years.

6. Conclusions and future work

In this study, a modelling approach was proposed to predict the carbonation depth. This approach is based on mechanisms of the $CO_{2(aq)}$ diffusion and $Ca(OH)_{2(aq)}$ reaction mechanisms in cementitious materials, in concrete exposed to carbon dioxide environment conditions. The following conclusions can be drawn from the results.

1- In models of carbonation depth, D_{CO2} considered internally affected factors such as the porosity and tortuosity of voids in concrete.

2- In the modelling of carbonation, the diffusion of carbon dioxide coefficient, D_{CO2} considered the impact of crack width and externally affected factors such as temperature and relative humidity.

3- An integrated carbonation model was developed to predict the depth of carbonation in non-pozzolanic, uncracked and cracked concrete specimens, considering properties of concrete, concentrations of CO_2, temperature and humidity together. The numerical model was verified by accelerated experimental results from this study and other studies for two cases of concrete, uncracked and cracked concrete samples.

4- The influence of climate change due to the increase in CO_2 and temperature and reduction in the relative humidity has a considerable impact on the depth of carbonation in the long term. This impact is much higher with an increase in the w/cm ratio due to an increase in the porosity and diffusivity of CO_2 in concrete structures.

5- There are two main cases of exposure environment, which can be investigated looking at two levels of CO_2 concentration according to the two worst scenarios of IPCC 2014, RCP 8.5 and RCP 6.0, which applied on concrete structures in London and those can be employed on other cities in the world in further studies.

6- Climate change could affect the progression of carbonation and induce corrosion in our concrete structures. Ultimate carbonation depths will be much higher in the long term and harsher exposure conditions such as the worst-case scenario of RCP 8.5.

7- Based on the IPCC 2014 climate change predictions, climate change appears to have an unnoticeable impact on the durability of concrete structures constructed in the Year 2000 in the short term; the significant effects of the climate change will become evident after approximately 30 years. Therefore, climate change mitigation measures should be put in place with the above predictions in mind to avoid expensive repair and maintenance costs in the future.

7. Appendix

Table A.1: Fresh and microstructure properties of mixes used in the study*

Mixes Designation	$\frac{w}{c}$	Slump mm	Density kg/m^3	Porosity %	Water absorption %	Compressive strength MPa
M 0.4	0.4	110	2467	10.01	4.6	51.5
M 0.5	0.5	130	2416	11.1	5.2	40.1
M 0.6	0.6	140	2389	12.3	5.7	36.3

Table A.2: Effect of CO_2 concentration on DoC for Scenario a*

Sample	w/binder	Crack width mm	Carbonation depth (mm) for Temperature 25 ºC, Relative humidity 65% and		
			CO_2=1.5% (7)	CO_2=3% (6)	CO_2=5% (5)
M 0.4	0.4	0	4	6	8
		0.05-0.15	14	16	19
		0.15-0.25	18	20	23
		0.25-0. 35	20	31	36
M 0.5	0.5	0	7.5	10	11.5
		0.05-0.15	18	20	26
		0.15-0.25	23	26	30
		0.25-0. 35	33	34	38
M 0.6	0.6	0	10	12	15
		0.05-0.15	22	23	26
		0.15-0.25	27	30	35
		0.25-0. 35	35	42	48

Table A.3: Effect of Temperature on DoC for Scenario b*

Sample	w/binder	Crack width mm	Carbonation depth (mm) for , Relative humidity 65% CO_2=5% and		
			Temperature 25 ºC (5)	Temperature 35 ºC (3)	Temperature 45 ºC (1)
M 0.4	0.4	0	8	9	9.5
		0.05-0.15	19	20	21
		0.15-0.25	23	25	23
		0.25-0. 35	36	35	36
M 0.5	0.5	0	11.5	13	13.5
		0.05-0.15	26	24	27
		0.15-0.25	30	29	31
		0.25-0. 35	38	40	42
M 0.6	0.6	0	15	16	17
		0.05-0.15	26	28	30
		0.15-0.25	35	35	33
		0.25-0. 35	48	50	47

Table A.4: Effect Relative humidity on DoC for Scenario c*

Sample	w/binder	Crack width mm	Carbonation depth (mm) for Temperature 25 ºC, CO_2=5% and		
			Relative humidity 65% (5)	Relative humidity 75% (4)	Relative humidity 85% (2)
M 0.4	0.4	0	8	7	5
		0.05-0.15	19	13	12
		0.15-0.25	23	21	20
		0.25-0. 35	36	30	32
M 0.5	0.5	0	11.5	11	10
		0.05-0.15	26	23	20
		0.15-0.25	30	29	23
		0.25-0. 35	38	40	37
M 0.6	0.6	0	15	15	14
		0.05-0.15	26	25	33
		0.15-0.25	35	36	38
		0.25-0. 35	48	46	50

*This means the results of these tests are an average for three sample

8. References

[1] Letcher, T. M. (2015). "Climate change: observed impacts on planet Earth". Elsevier.

[2] Clarke, L. Dahe, Q.and Dasgupta, P. (2014). "Climate change 2014: synthesis report. Contribution of Working Groups I, II and III to the fifth assessment report of the Intergovernmental Panel on Climate Change", IPCC-2014.

[3] UKCP'09,(2010). " UK Climate Projections science report: Climate change projections". [Online] Available at http://ukclimateprojections.defra.gov.uk.pdf.

[4] Bernstein, L., P. Bosch, O. Canziani, Z. Chen, R. Christ, O. Davidson, W. Hare, S. Huq, D. Karoly and V. Kattsov (2008). "Climate change 2007: Synthesis report: An assessment of the intergovernmental panel on climate change", IPCC-2007.

[5] Hussain, S., A. Al-Musallam and A. Al-Gahtani (1995). "Factors affecting threshold chloride for reinforcement corrosion in concrete". Cement and Concrete Research 25(7): 1543-1555.

[6] Tuutti, K. (1982). " Corrosion of steel in concrete". Stockholm, Swedish Cement and Concrete Research Institute.

[7] Lagerblad, B. (2005). "Carbon dioxide uptake during concrete life cycle–state of the art". Swedish Cement and Concrete Research Institute CBI, Stockholm.

[8] Broomfield, J. P. (2007). "Corrosion of steel in concrete: understanding, investigation and repair ". Taylor &Francis.

[9] Tarun, R. and K. Rakesh (2010). "Global warming and cement-based materials ". UWM Center for By-Products Utilization.

[10] Talukdar, S., N. Banthia and J. Grace (2012). "Carbonation in concrete infrastructure in the context of global climate change–Part 1: Experimental results and model development". Cement and Concrete Composites 34(8): 924-930.

[11] Lea, F. M. (1971). "Some Special Cements and Cement Properties". The Chemistry of Cement and Concrete, Chemical Publishing Company, NY, U.S.A., Chapter 17, 544-547.

[12] Dyer, T. (2014). "Concrete durability". Crc Press.

[13] International Federation for Structural Concrete, CEB-FIP (2013). "Model Code for Concrete Structures 2010". Wilhelm Ernst & Sohn, Verlag für Architektur und technische Wissenschaften GmbH & Co. KG, Rotherstraße 21, 10245 Berlin, Germany.

[14] Yoon, I.-S., O. Çopuroğlu and K.-B. 19 (2007). "Effect of global climatic change on carbonation progress of concrete". Atmospheric Environment 41(34): 7274-7285.

[15] Park, D. (2008). "Carbonation of concrete in relation to CO_2 permeability and degradation of coatings". Construction and Building Materials 22(11): 2260-2268.

[16] Kwon, S.-J. and Na, U.-J. (2011). "Prediction of durability for RC columns with crack and joint under carbonation based on probabilistic approach". International Journal of Concrete Structures and Materials 5(1): 11-18.

[17] Drouet, E., Poyet, S., Le Bescop, P., Torrenti, J.M. and Bourbon, X.,(2019) "Carbonation of hardened cement pastes: Influence of temperature". Cement and Concrete Research, 115(2019) 445-459.

[18] Roy, S, Poh, K and Northwood, D.,(1999) "Durability of concrete accelerated carbonation and weathering studies", Building and Environment, 34 (5) (1999) 486-595.

[19] European Committee for Standardization, BS EN 197-part 1(2011). "Cement: Composition, specifications and conformity criteria for common cements". British Standard Institution.

[20] European Committee for Standardization, BS EN 12620:2002+A1:2008." Aggregate for concrete". British Standard Institution.

[21] American Society for Testing and Materials, ASTM C642:2013, "Density, Absorption, and Voids in Hardened Concrete".

[22] European Committee for Standardization, BS EN 12390, part 3(2000). "Testing hardened Concrete. Compressive strength of test specimens". British Standard Institution.

[23] European Committee for Standardization, CEN/TS 12390-10(2007). "Testing hardened concrete: Determ9ination of the carbonation resistance of concrete at atmospheric levels of carbon dioxide". British Standard Institution.

[24] Castellote, M., Fernandez, L., Andrade, C., & Alonso, C. (2009). Chemical changes and phase analysis of OPC pastes carbonated at different CO 2 concentrations. Materials and Structures, 42(4), 515-525.

[25] Glasser FP, T. Matschei. Interactions between Portland cement and carbon dioxide. In: Proceedings of the 12th ICCC. Montreal, Canada; 2007.

[26] Neville, A. M. (2011). "Properties of Concrete ". 5th edition. London, Pearson Education Limited.

[27] Al-Ameeri, A., K. AL-Hussain and M. Essa (2013). "Predicting a Mathematical Models of Some Mechanical Properties of Concrete from Non-Destructive Testing." Civil and Environmental Research 3: 78-97.

[28] AL-Ameeri, A., R. AL-Rawi (2009). " A Study on Properties of Iraqi Steel slag as a Fine Aggregate in Concrete ". Journal of Building Technology, Saudi Arabia 13/2009.

[29] American Code Institute, ACI Committee 122 R. (2002). "Guide to thermal properties of concrete and masonry systems".

[30] Papadakis, V. G., C. G. Vayenas and M. N. Fardis (1991). "Fundamental modeling and experimental investigation of concrete carbonation". Materials Journal 88(4): 363-373.

[31] Papadakiss, V.G., S.Tsimas, (2002). " Supplementary cementing materials in concrete Part I: efficiency and design". Cement and concrete research 32(2002): 1525-1532.

[32] He, R. 2010. A study on carbonation for low calcium fly ash concrete under different temperature and relative humidity. The Electronic Journal of Geotechnical Engineering (EJGE), 15, pp.1871-1877.

[33] Song, H.-W., S.-J. Kwon, K.-J. Byun and C.-K. Park (2006). "Predicting carbonation in early-aged cracked concrete". Cement and Concrete Research 36(5): 979-989.

[34] Smilauer, V., L. Jendele and J. Cervenka (2013). "Prediction of Carbonation and Chloride Ingress in Cracked Concrete Structures". BHV Topping and P. Iványi, Editors. Proceedings of the Fourteenth International Conference on Civil, Structural and Environmental Engineering Computing.

[35] Fogg, P. G., J. Sangster, Y.-N. Lee, S. Schwartz and P. Warneck (2003). "Chemicals in the atmosphere: solubility, sources and reactivity ". Wiley Chichester.

[36] Ishida, T., T. Kishi and K. Maekawa (2014). " Multi-scale modeling of structural concrete ". Crc Press.

[37] Khunthongkeaw, J. and S. Tangtermsirikul (2005). "Model for simulating carbonation of fly ash concrete". Journal of materials in civil engineering 17(5): 570-578.

[38] Cook, R. D. (2007). "Concepts and applications of finite element analysis". John Wiley & Sons.

[39] Ngo, D. and A. C. Scordelis (1967). "Finite element analysis of reinforced concrete beams". Journal Proceedings, 64(3): 152-163.

[40] Chang, C.-F. and J.-W. Chen (2006). "The experimental investigation of concrete carbonation depth". Cement and Concrete Research 36(9): 1760-1767.

[41] Ehrlich, H. L., D. K. Newman and A. Kappler (2015). "Ehrlich's geomicrobiology ". CRC press.

[42] Chi, J. M., R. Huang and C. Yang (2002). "Effects of carbonation on mechanical properties and durability of concrete using accelerated testing method". Journal of marine science and technology 10(1): 14-20.

[43] AL-Ameeri, A., Rafiq, M., O. Tsioulou (2019). "Effect of Cracks on Alkalinity Level of Concrete Structure Exposed to CO2 Environment Conditions". Euro Coal Ash, June 2019-Dundee - Scotland.

[44] AL-Ameeri, A., Rafiq, M. and O. Tsioulou (2018). "Influence of Cracks on the Carbonation Resistance of Concrete Structure". Sixth International Conference on Durability of Concrete Structures (ICDCS 2018), 18-20 July 2018, Leeds – UK.

[45] AL-Ameeri, A.S., Rafiq, M.I. and O. Tsioulou (2020). "Combined impact of carbonation and crack width on the Chloride Penetration and Corrosion Resistance of Concrete Structures". Cement and Concrete Composites, p.103819.

[46] Talukdar, S., N. Banthia, J. Grace and S. Cohen (2012-a). "Carbonation in concrete infrastructure in the context of global climate change: Part 2–Canadian urban simulations". Cement and Concrete Composites 34(8): 931-935.